

Removal of tetracyclines from aqueous solutions by electrocoagulation/pecan nutshell coupling processes: synergistic effect and mechanism

Kunkun Xiao, Dongmei Huang, Chunli Kang and Siyang Sun

ABSTRACT

The present work compared electrocoagulation (EC)/pecan shell (PS) coupling process with a simple electrocoagulation (EC) process for the removal of tetracyclines (TCs). The results indicated that the addition of appropriate PS could lead to the enhancement of the removal efficiency and decrease of operating time via synergistic influence, including conventional EC process, biomass materials adsorption, charge neutralization and coordination adsorption. The ideal condition for the coupling process was 2.5 mA/cm² for current density and 3 cm for plate spacing. Based on the optimum condition, when the dosage of PS was 5 g/L, the initial concentration of tetracycline hydrochloride (TC), oxytetracycline hydrochloride (OTC) and chlortetracycline hydrochloride (CTC) was 250 mg/L, the removal rate of PS was 55.90%, 45.10% and 14.98% higher than those of EC process after 40 min treatment. In addition, compared to conventional EC process, the unit energy demand (UED) decreased by 49.62%, 53.24% and 26.35% and the unit electrode material demand (UEMD) decreased by 49.80%, 85.65% and 44.37%, respectively, which means more energy conservation and environmental protection.

Key words | adsorption, electrocoagulation, pecan shell, tetracyclines

Kunkun Xiao
Dongmei Huang
Chunli Kang (corresponding author)
Siyang Sun
 Key Laboratory of Groundwater Resources and Environment, Ministry of Education, Jilin University, Changchun 130012, China
 E-mail: kangcl@jlu.edu.cn

HIGHLIGHTS

- Electrocoagulation (EC)/pecan shell (PS) coupling process could purify tetracyclines (TC, OTC and CTC) solution with high concentration in a short time.
- X-ray photoelectron spectroscope (XPS) was used to investigate the mechanism of EC+PS process.
- The sedimentation of floccules produced in EC+PS system could be promoted by PS.
- EC+PS coupling process is an efficient and cheaper technique for TCs removal.

INTRODUCTION

Antibiotics have been extensively used for human and veterinary therapeutic purposes (Javid *et al.* 2016; Song 2016). The amount of antibiotics used each year has reached up to 100,000–200,000 tons globally, with more than 25,000 tons in China annually (Yan *et al.* 2013). The most commonly used tetracyclines (TCs) include tetracycline hydrochloride (TC), oxytetracycline (OTC) and chlortetracycline (CTC) (Ji *et al.* 2016). However, only partially TCs can be metabolized by human and animals and

unabsorbed residues will be released into the environment. Hence, the overuse of these compounds results in the pollution of the environment eventually. In China, tetracycline antibiotic residues have been detected in many water bodies, such as the Yangtze River Basin, Songhua River Basin, Poyang Lake Basin, Haihe River Basin and Three Gorges Reservoir area (Luo *et al.* 2011; Wang *et al.* 2017a, 2017b). Residues of TCs are also found in the aquatic environment in the United States

(Karthikeyan & Meyer 2006), Iran (Javid *et al.* 2016) and other countries. Such antibiotics can cause chronic poisoning of aquatic organisms, and will be partly absorbed and then accumulated by plants when they enter the soil. Finally, they will cause harm to human body through the food chain, and enhance the antibiotic resistance of microorganisms via generating resistance genes (Wan *et al.* 2010).

At present, TC antibiotics effluent is commonly purified by physicochemical and biological treatment, and anaerobic process in biological methods is preferred in general (Shi *et al.* 2017). However, considering the relatively high residues in TCs wastewater, physicochemical method should be used for pretreatment before biological treatment. There are various physical, chemical or biological processes for TCs contaminated waters, such as coagulation-sedimentation, adsorption, flotation, osmosis, micro electrolysis and photo-Fenton process, etc. (Kakavandi *et al.* 2016; Antonherero *et al.* 2017; Barthoumi *et al.* 2017; Saitoh *et al.* 2017; Zhang *et al.* 2017; Khanday & Hameed 2018; Zhang *et al.* 2018). Other than the above mentioned processes, electrocoagulation (EC), electrooxidation and electrofloatation in electrochemistry area are also available as relatively new technologies. Electrocoagulation combines the advantages of coagulation, flotation and electrochemistry, becoming an emerging technology in water and wastewater treatment. EC is one kind of treatment techniques that is capable of being clean, easyhandling and high efficiency in the removal of organic pollutants (Moussa *et al.* 2017). In consideration of the shortcomings of traditional electrocoagulation, including easy passivation of electrodes, low efficiency, high energy consumption, it has become a hot research area to combine electrocoagulation technology with other technologies to improve the treatment efficiency and reduce the treatment cost. E. Hernández-Francisco combined electroflocculation-Fenton/photo-Fenton technologies to treat phenolic pollutants in refinery effluents, and the final total organic carbon (TOC) removal rate reached 88% (Hernández-Francisco *et al.* 2017); Marius Sebastian Secula removed acid dyes from wastewater by electroflocculation/biochar adsorption coupling, which improved the removal rate of indigo carmine in aqueous solutions and reduced the adsorption time and energy consumption (Secula *et al.* 2012).

The main aim of this work is to investigate the efficiency and the mechanism of the electrocoagulation technique coupling with PS for removing TCs from aqueous solution. It may provide a highly effective technology to treat high concentration TCs effluents.

MATERIALS AND METHODS

Materials

PS powder was purchased from Meihokou Tiancheng Food Company, dried at 60 °C for 24 h and sieved with a 80 mesh. Tetracycline hydrochloride ($C_{22}H_{24}N_2O_8 \cdot HCl$, MW = 480.9 $gmol^{-1}$, USP grade, $\geq 98\%$), oxytetracycline hydrochloride ($C_{22}H_{24}N_2O_9 \cdot HCl$, MW = 496.89 $gmol^{-1}$, USP grade, $\geq 95\%$), chlortetracycline hydrochloride ($C_{22}H_{23}ClN_2O_8 \cdot HCl$, MW = 515.34 $gmol^{-1}$, USP grade, $\geq 80.0\%$) and sodium sulphate ($NaSO_4$, AR) were purchased from Shanghai Aladdin Bio-Chem Technology Co.

Characterization of adsorbent

Scanning electron microscope (SEM) measurements were performed by a field emission scanning electron microscope (Hitachi, S-4800). Fourier transform infrared spectrum (FTIR) was used to verify the change of the bonds on a SHIMADZU Irfaffinity-1S spectrophotometer using KBr as a diluent. The method of the point of zero charge (pzc) in this work is as follows. In each of the 50 mL bottles, 40 mL of water is added, and the pH is adjusted with 0.1 mol/L HNO_3 ranging from 2 to 10. Then 100 mg of PS powder is added and the final pH of the solution is measured after vibrating at the constant temperature for 24 h. When the initial and final pH values are equal, the initial pH is the point of zero charge. After flocculation, flocs are carefully withdrawn from the bottom of jars, and then vacuum freeze-dried to prevent the change of functional groups in flocs.

Experimental method

As shown in Figure 1, the experiment was conducted in an electrocoagulation cell (15 cm \times 11.9 cm \times 15.6 cm). The bottom of the cell was equipped with six perforated tubes which connected to an air pump to provide agitating aeration. The electro-chemical setup was constituted with an aluminum plate as the anode and a stainless steel plate as the cathode. Aluminum and stainless steel are widely used in the process of electric flocculation, because the multivalent ion coagulation effect produced by the multivalent electrode used as the anode is economical and common. Aluminum and stainless steel plates can be used as a single electrode or in combination, and the flocculation produced in combination has a higher flocculation effect. The electrodes were connected to a digital DC power supply

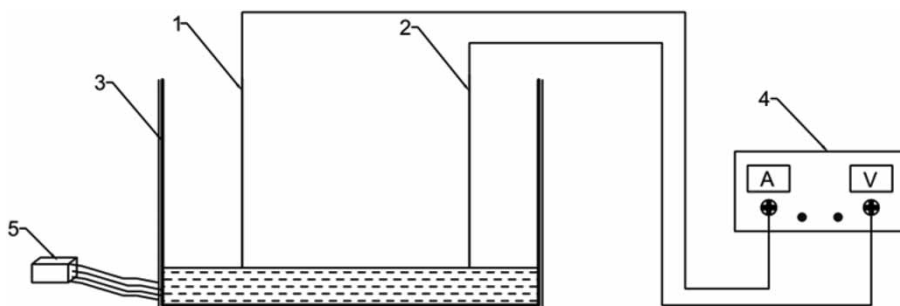


Figure 1 | EC experimental set-up: 1- anode (aluminum); 2- cathode (stainless steel); 3- reactor; 4- DC power supply; 5- aquarium air pumps.

(WYJ, 0–30 V; 0–5 A; DC Regulated Power Supply Double Way Output, TESTMART, Shanghai, China). The effective electrode area was 36 cm².

For every experimental run, 800 mL of TCs solution (250 mg/L) was placed into the reactor and 1 g/L Na₂SO₄ solution was added to adjust the conductivity. The current density and electrode space were set to a desired value and then a certain quantity of PS was added to the solution. To assess the treatment process, 5 mL water sample was drawn every 5 min during the experiment. The samples were filtered through Whatman 0.45 μm filters, and then measured with a UV-vis spectrophotometer (UVmini-1240, Shimadzu). The maximum absorption wavelength of TC, OTC, and CTC were 356, 354 and 365 nm, respectively. The influencing factors were also investigated, containing the plate spacing, current density, walnut shell dose and initial concentration of TCs.

Unit energy and electrode material demand

Energy consumption is one of vital parameters for the feasibility of the electrochemical process. Unit energy demand (UED) is the electrical energy required to remove pollutants per kilogram. The experiments were carried out in a galvanostatic regime and UED was calculated according to Equation (1):

$$\text{UED} = \frac{I \cdot \int_0^t U \cdot dt}{V \cdot C_0 \cdot \frac{Y_t}{100}} \quad (1)$$

where U is the cell voltage, (V); I is current intensity, (A); t is time, (h); V is volume of TCs solution, (L); Y_t is removal efficiency at time t, (%); C₀ is initial concentration of TCs in solution.

The generation of the coagulant during the EC process leads to the consumption of the electrode material. Unit

electrode material demand (UEMD) is the electrode material consumed to remove pollutants per kilogram and UEMD was calculated according to Equation (2):

$$\text{UEMD} = \frac{3600 \cdot I \cdot t \cdot A}{n \cdot F \cdot V \cdot C_0 \cdot \frac{Y_t}{100}} \quad (2)$$

where I is the current intensity, (A); t is time, (h); n is number of electrons involved in the oxidation/reduction reaction; F is Faraday's constant, (C/mol); A is atomic mass of the electrode material, (g/mol); Y_t is removal efficiency at time t, (%); C₀ is initial concentration of TCs in solution, (g/L); and V is volume of TCs solution, (L).

RESULTS AND DISCUSSION

Characterization of materials

SEM analysis

Figure 2 reveals the SEM images of PS morphology; the PS appears to have a rough surface with irregular pores. The distinct gullies on the surface could increase the specific surface area, which facilitates the contact between PS and target pollutant molecules.

FTIR analysis

FTIR spectrum of PS was illustrated in Figure 3. For PS, the major intense bands were at 3,415.03 cm⁻¹ (-OH stretching); 2,933.78 cm⁻¹ (attributed to C-H stretching vibration in aliphatics); 1,735 cm⁻¹ (C=O stretching vibration in hemicellulose); 1,264.36 cm⁻¹ (C-O-C stretching vibration in cellulose) and 1,047 cm⁻¹ (C-O stretching vibration). The specific bands at 1,500–1,300 cm⁻¹ was owing to O-H stretching vibration, the deformation of a methoxy group

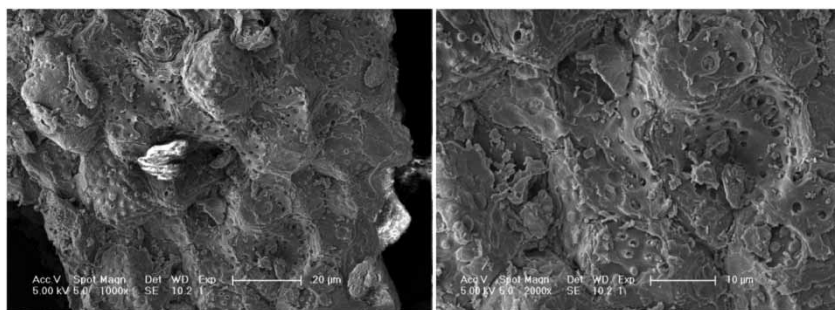


Figure 2 | SEM images of PS.

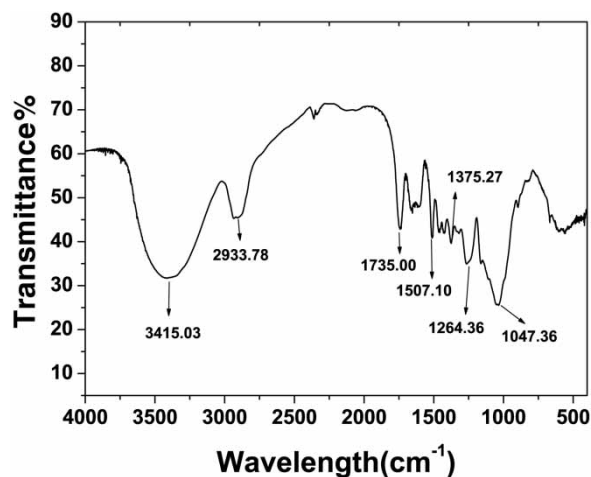


Figure 3 | FTIR spectrum of PS.

in lignin structure and aliphatic CH_2 group in cellulose structure (Xu *et al.* 2013). Hence, it can be concluded that there are characteristic functional groups on the surface of PS, which may interact with the substances in the EC + PS system via charge or hydrogen bond.

pH_{pzc} of PS

pH_{pzc} is the pH at which the surface exhibits net zero charge. The results show that the pH_{pzc} of PS is approximately 5.0 (Figure 4), meaning that when the pH is less than 5.0, PS has a positive charge, and opposite charge would be obtained at pH > 5.0.

RESULTS AND MECHANISM OF TC REMOVAL

Removal of different TCs

Figure 5 shows the effects of EC + PS coupling method on the removal of TC (a), OTC (b) and CTC (c). PS adsorption

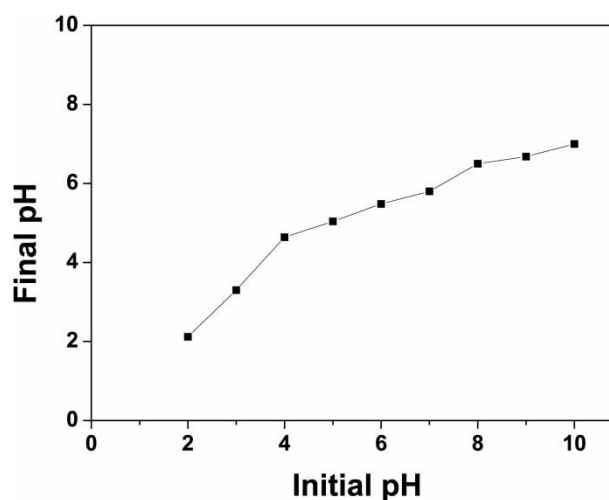


Figure 4 | pH_{pzc} result of PS.

process and EC were used as controls, respectively. The order of removal rate of TCs for different systems is EC + PS > EC >> PS. Individual EC system can also reach a relatively high removal rate if the reaction time is long enough. Therefore, compared to EC system, the enhanced treatment effect of EC + PS system was mainly reflected in the decrease of reaction time, meaning a higher reaction rate. The following relationship of the removal rate on TCs at 40 min has been acquired: TC:PS (3.02%) + EC (36.32%) < EC + PS (89.90%); OTC:PS (4.32%) + EC (35.87%) < EC + PS (76.00%); CTC:PS (5.73%) + EC (13.13%) < EC + PS (50.78%). Thus the removal of TCs by EC + PS coupling process is not a simple addition of EC process and PS adsorption process, while there is a synergistic effect existing during the whole EC + PS coupling procedure. According to the comparison in Figure 5(a)–5(c), the order of removal rate of tetracyclines is CTC > TC > OTC, which is attributed to their different molecular structure. Yuanzhu Li studied dissipation kinetics of OTC, TC, and CTC residues in soil, and found the stability order of

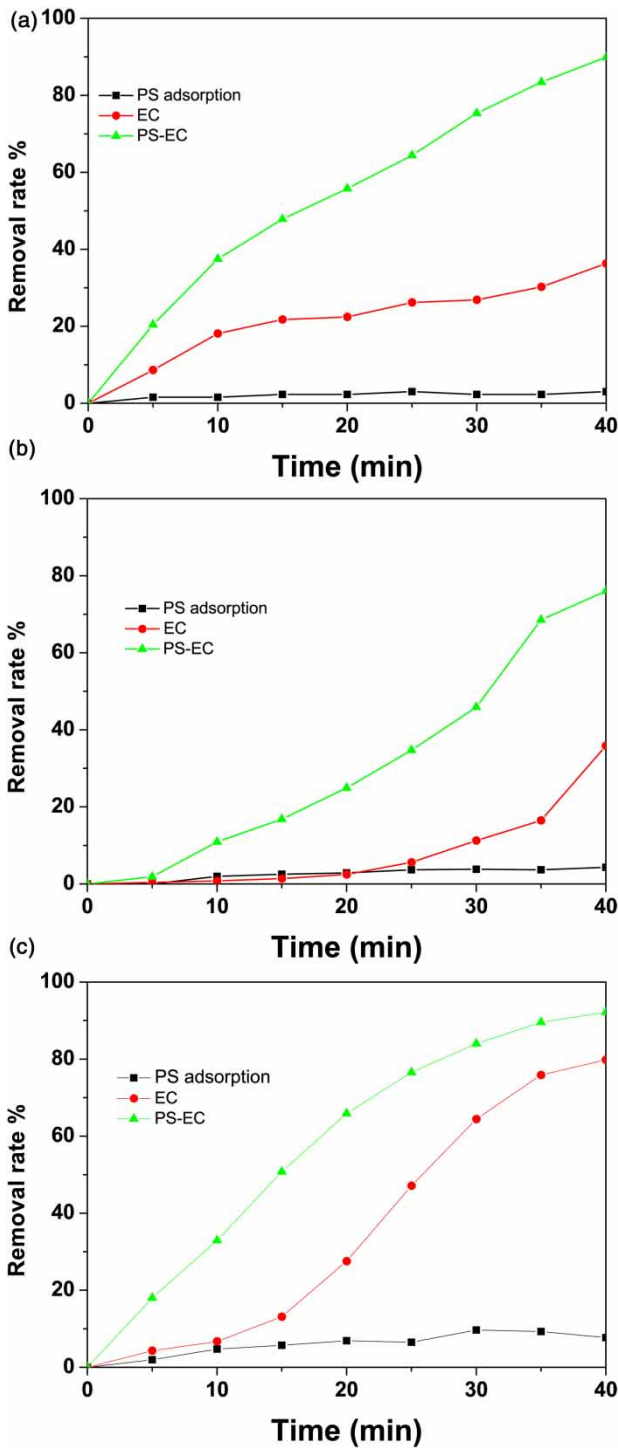


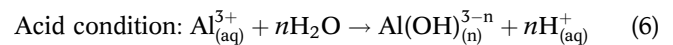
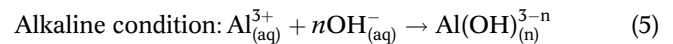
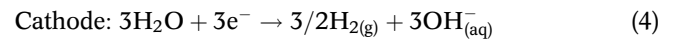
Figure 5 | Removal of three TCs (a) TC, (b) OTC, (c) CTC by EC + PS coupling method.

the three TCs was OTC > TC > CTC, which was consistent with the result of our experiments (Li et al. 2016). Wanru Chen investigated the adsorption and transformation of tetracycline antibiotics with aluminum oxide, and the

reactivity towards Al_2O_3 followed the order of $\text{CTC} > \text{TC} > \text{OTC}$ (Chen & Huang 2010).

Mechanism analysis

The proposed mechanism for the generation of coagulation by using of Al as an anode is presented below.



It can be seen from the reaction equations that metal ions are generated by anodic dissolution (Equation (3)), and then form a series of mononuclear or multinuclear metal hydroxy complexes in the electrolytic cell, such as $\text{Al}(\text{OH})_2^+$, $\text{Al}(\text{OH})_2^+$, $\text{Al}_2(\text{OH})_2^{4+}$, $\text{Al}(\text{OH})_4^-$, $\text{Al}_6(\text{OH})_{15}^{3+}$, $\text{Al}_7(\text{OH})_{17}^{4+}$, $\text{Al}_8(\text{OH})_{20}^{4+}$, $\text{Al}_{13}\text{O}_4(\text{OH})_{24}^{7+}$, $\text{Al}_{13}(\text{OH})_{34}^{5+}$, and finally $\text{Al}(\text{OH})_3$ (s) would be formed through a complex precipitation kinetic procedure (Equations (5) and (6)). All these Al containing components have a large surface area, and is conducive to the rapid adsorption of TCs and the capture of colloidal particles in aqueous, which is finally removed by precipitation. The mechanism of coupling methods is just the addition of electrocoagulation and adsorption of biomass materials in electrocoagulation coupled with banana peel, rice husk and other materials (De Carvalho et al. 2015; Wang et al. 2017a). But in our coupling systems, there is also a synergistic effect throughout the TC antibiotics removal process.

In EC + PS coupling system, PS would have different kind of charge at different pH value (Figure 4). According to the fact that the initial pH of the solution is between 3.5 and 3.6, yet the final pH is between 6.7 and 6.9, the PS was first positively charged and then negatively charged during the whole treatment process, which led to the enhanced TCs removal because charge neutralization would occur between the PS with negative charge and the TCs ion with positive charge.

The chemical state and composition of elements of the flocculate acquired from different systems was analyzed using X-ray photoelectron spectroscope (XPS). Figure 6 shows the results of XPS analysis for PS and the flocculates obtained in EC + PS and EC + PS + TC systems. C1s peak for PS can be deconvoluted into two peaks at binding

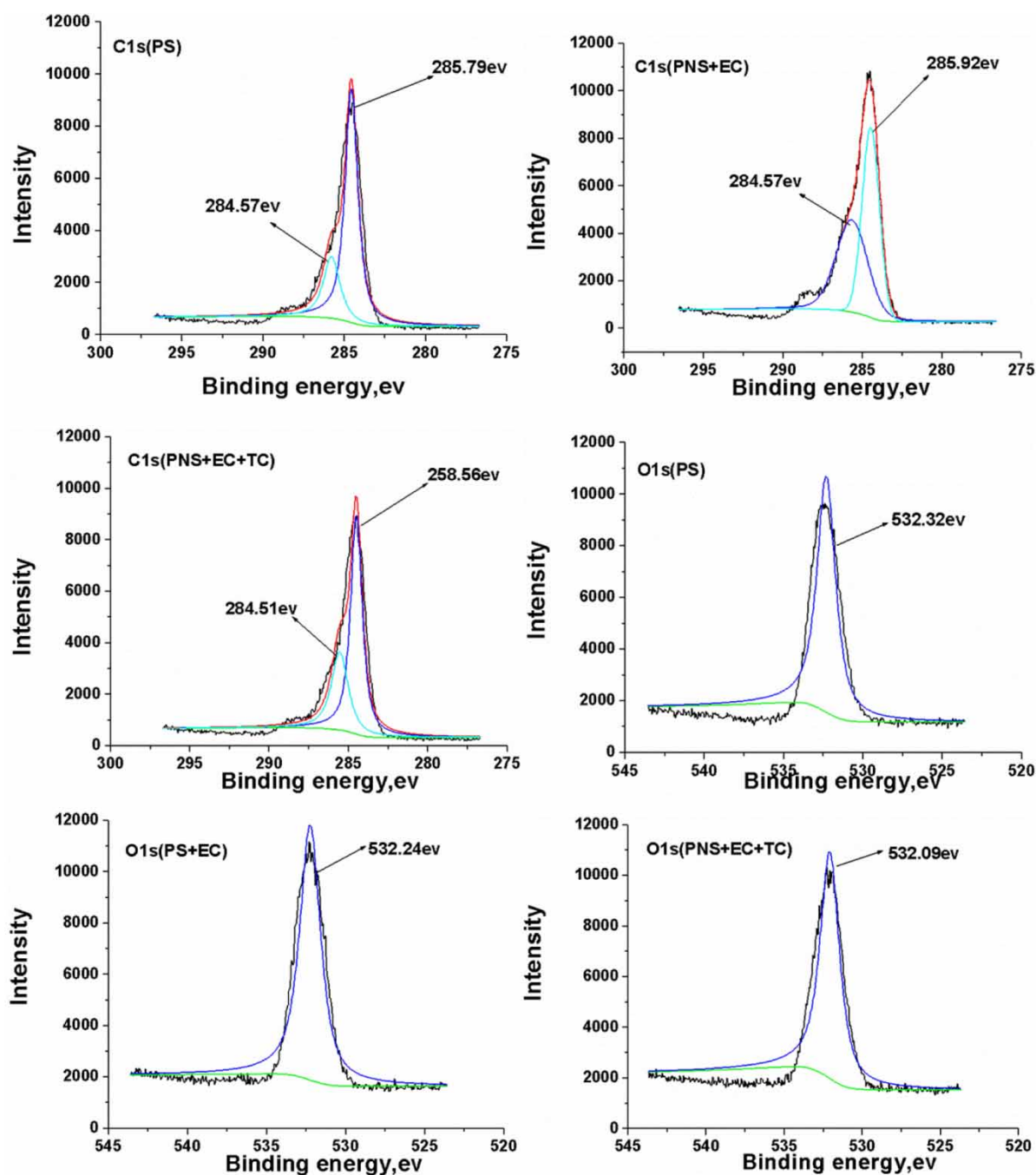


Figure 6 | XPS spectra of C1s and O1s of PS samples in different treatment process.

energies of ~ 284.57 and 285.79 eV, respectively. The former can be associated with C = C bonding (Chen & Huang 2010), and the latter is assigned to C-N bonding (Wei *et al.* 2016). In EC + PS system, the peak at 284.57 eV does not shift, but the peak at 285.79 eV has transferred to 285.92 eV (C-N binding), because Al^{3+} produced in EC + PS process could coordinate with C-N functional group. Compared to

EC + PS system, the two peaks generated by the flocculate in EC + PS + TC system shift more obviously. The peak representing C = C bond shifts a little from 284.57 to 284.51 eV, probably attributed to the weak interaction between TC and C = C. The peak representing C-N moves more largely from 285.79 to 285.56 eV, which is due to the coordination between Al^{3+} , C-N and TC. For PS, there is a

peak of O1s at the binding energy 532.32 eV, while it has transferred to 532.24 eV in PS + EC system and 532.09 eV in EC + PS + TC system, respectively. It can be inferred that the peak shift results from the coordination of Al^{3+} with C=O firstly and then, with TC molecules. Therefore, according to XPS analysis, the Al^{3+} produced in the EC process could coordinate with C-N and C=O on the surface of biomass materials, which would further coordinate with TC to form larger particles, so as to improve the flocculation performance and accelerate the removal of pollutants. PS plays a role of 'bridging' throughout the whole removal procedure. Shuying Jia *et al.* believed that Cu (II) can further interact with tetracycline after coordination with C-N and C=O of the flocculant and enhance the flocculation effect, when they studied the removal of coexisting Cu (II) and TC using aromatic functionalized chitosan flocculant (Jia *et al.* 2016). This conclusion was in accordance with our work. Therefore, charge neutralization and coordination adsorption are the main reasons for the synergistic effect of EC + PS + TC system.

EFFECTS OF CURRENT DENSITY

Current density (CD) is an important parameter for controlling the electrochemical reaction rate. CD can be formulated as:

$$\text{CD} = I/S \quad (7)$$

where CD is the current density (Acm^{-2}), I is the current (A), and S is the total area of anode (cm^2).

The effect of current density (2.5, 5, 7.5 and 10 mA/cm^2 , respectively) on the removal rate of TC in water was shown in Figure 7. The removal efficiency of TC increased with the current density increasing in EC and EC + PS process. When CD became higher, the anodic dissolution of Al increased, which leads to an increase in the amount of metal hydroxides as well as an improvement of removal efficiency. But if the reaction time is enough, increasing the current density could speed up the removal rate and has little effect on the final removal rate. Compared Figure 7(a) with 7b, the highest efficiency enhanced of TC removal by PS was obtained at low current density values of 2.5 mA/cm^2 . According to Equation (1), the energy consumption in condition of 2.5 mA/cm^2 with PS after 40 min is lowest among all conditions. Taking energy saving into consideration, the current density of 2.5 mA/cm^2 was chosen as ideal condition in subsequent experiments.

Effects of plate spacing

Figure 8 shows the influence of plate spacing (3, 6, 9 and 12 cm) on TC removal in EC and EC + PS processes. In the EC process for 40 min (Figure 8), the change of plate spacing has little effect on the removal process, yet between 40 and 60 min, the removal rate is highest when the plate spacing is 12 cm. It is mainly because the floc volume of aluminum hydroxides produced gradually increases with the reaction going on, and the large plate spacing is conducive to the full contact between the flocculate and TC. In EC + PS process (Figure 8(b)), the plate spacing has little effect on the removal rate. This is attributed to the existence of PS in the coupling system which promotes the uniform distribution of Al in the system, makes Al^{3+} fully contact

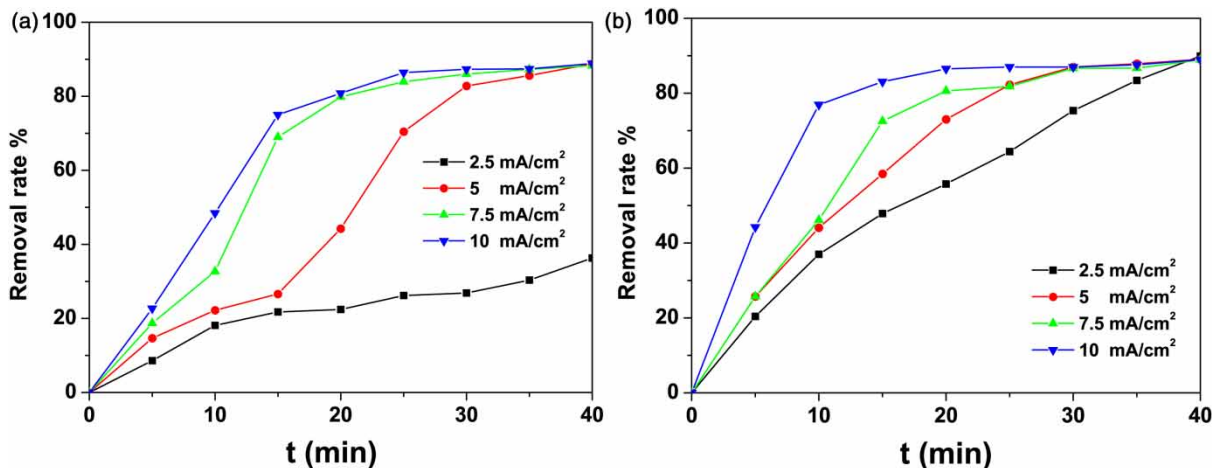


Figure 7 | Removal rate of TC at different values of current density. (a) EC, (b) EC + PS, [plate spacing] = 3 cm, [TC] = 250 mg/L, [PS] = 5 g/L.

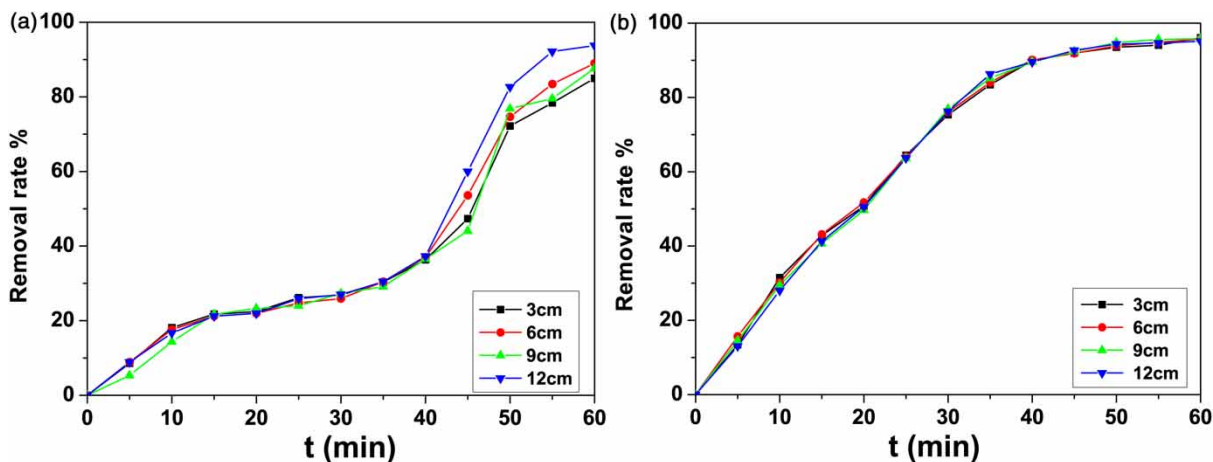


Figure 8 | Removal rate of TC at different plate spacing. (a) EC, (b) EC + PS, [CD] = 2.5 mA/cm², [TC] = 250 mg/L, [PS] = 5 g/L.

with TC and reduces the influence of changing plate spacing. The larger the plate spacing is, the greater the voltage in the reaction tank is, and the more energy would be consumed in the treatment process. Therefore, 3 cm is selected as the best plate spacing in the experiment.

Effects of PS dosage

Figure 9 compared the removal efficiencies of TCs for simple EC and EC-PS coupling system at different PS dosages. With the PS dosage increasing from 1 to 8 g/L at 40 min, the removal rate of TC was 66.70%, 77.80%, 89.90%, 91.30% and 92.20%, respectively. The greatest enhancement of PS-EC process over TCs occurred at 40 min (Figure 9(a)), because the removal rate of TC in EC-PS system could be increased by 55.90%, compared to the pure EC treatment (36.30%). The influence of PS dosage on the removal of OTC and CTC was similar to that of TC (Figure 9(b) and 9(c)). Taking into the operating cost of electrocoagulation process, 5 g/L was selected as the best dosage of pecan shell.

Effects of initial TC concentrations

The effect of initial concentration of TCs on the removal efficiency of the coupling method was investigated in Figure 10. The removal rate of TC decreased with the increase of TC concentration. Such results were attributed to the ability of the whole system to treat pollutants was limited under specific current density, PS dosage and reaction time. With the increase of the initial concentration, the removal rate of TC decreases beyond the range of the treatment ability.

For the three kinds of TCs (TC, OTC and CTC) with the initial concentration of 250 mg/L, the removal rate could reach 89.90%, 82.92% and 93.85% at 40 min, respectively.

Unit energy demand (UED) and unit material demand (UEDM) analysis

Figure 11 shows the effect of different doses of PS on the UED and UEMD in PS + EC system at different reaction time, 20 and 40 min are selected, respectively. At 20 and 40 min, the UED and UEMD decreased gradually with the increase of PS dosage, and decreased much more at 20 min than 40 min which indicated that PS-EC system had more prominent energy-saving influence in a short time. At the dosage of 5 g/L and reaction time of 40 min, the removal rate reached a high level and UED and UEMD of TC, OTC and CTC decreased obviously: UED decreased by 49.62%, 53.24%, 26.35% and UEMD decreased by 60.60%, 36.68%, 6.62%, respectively. Therefore, in PS-EC coupling treatment system, TCs can be effectively removed, and the UED and UEMD could also be significantly reduced, which means lower consumption of energy and electrode materials.

CONCLUSION

The optimal conditions for EC + PS coupling process were as follows: current density was 2.5 mA/cm², plate spacing was 3 cm and reaction time was 40 min. Under the best experiment condition, the removal efficiency of TC, OTC and CTC with initial concentration of 250 mg/L could

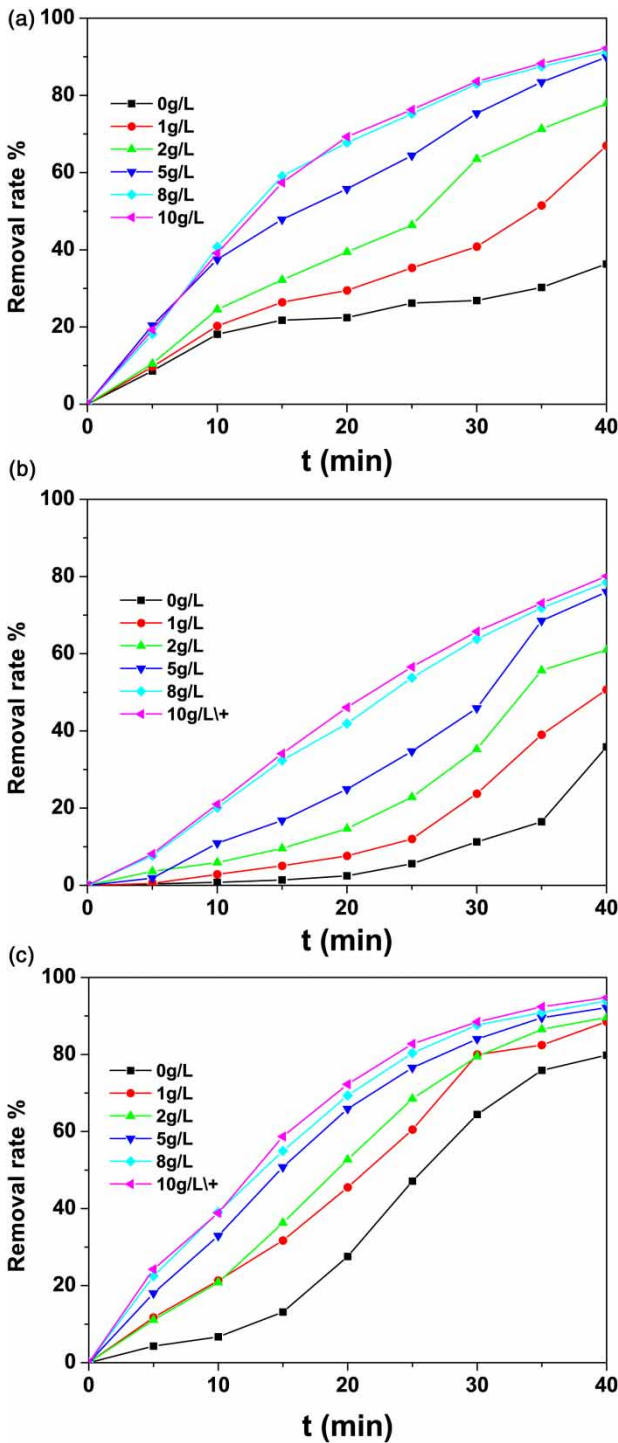


Figure 9 | Removal rate of (a) TC, (b) OTC and (c) CTC at different doses of PS. ([plate spacing] = 3 cm, [TC] = 250 mg/L, [CD] = 2.5 mA/cm²).

reach 89.90%, 82.92% and 93.85%, respectively. Compared with EC process, the removal efficiency in EC-PS system could be increased by 55.90%, 45.10% and

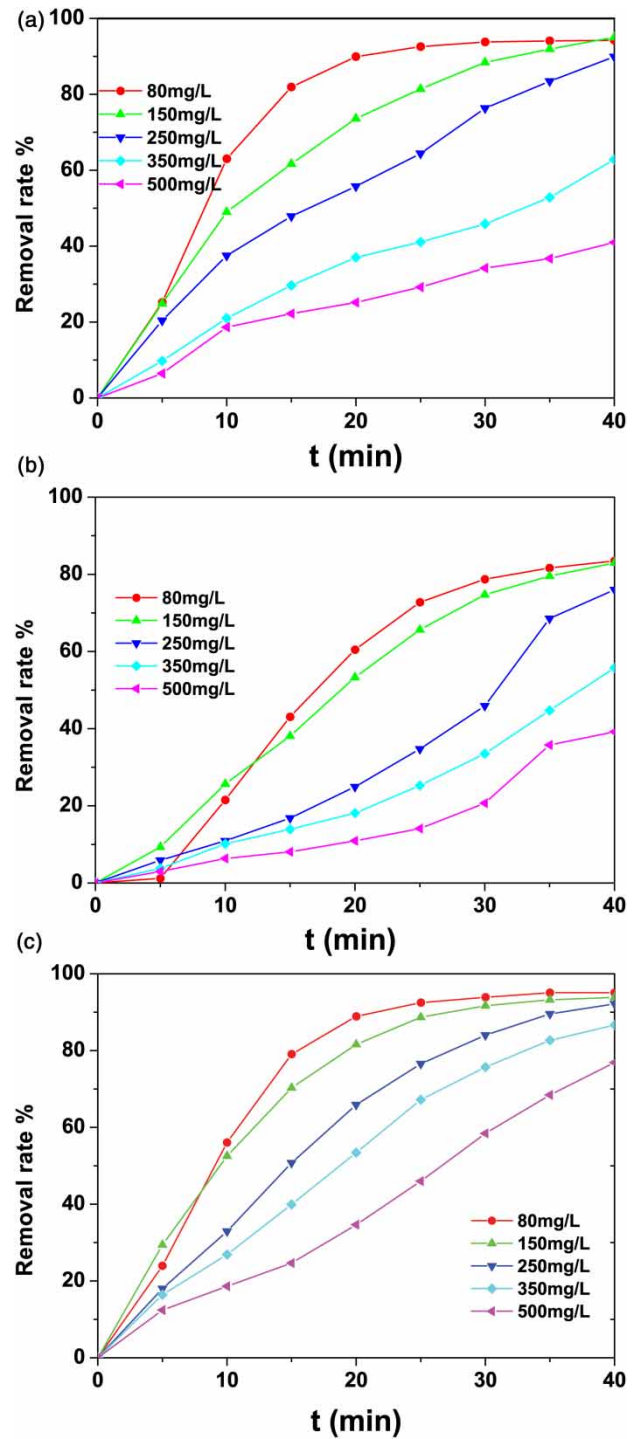


Figure 10 | Removal rate of TC at different initial TCs concentration. (a) TC, (b) OTC, (c) CTC, [CD] = 2.5 mA/cm²; [plate spacing] = 3 cm, [PS] = 5 g/L.

14.98%, respectively; the UED of the treatment process could be reduced by 49.62%, 53.24% and 26.35%, and the UEMD could be reduced by 49.35%, 80%, 85.65%,

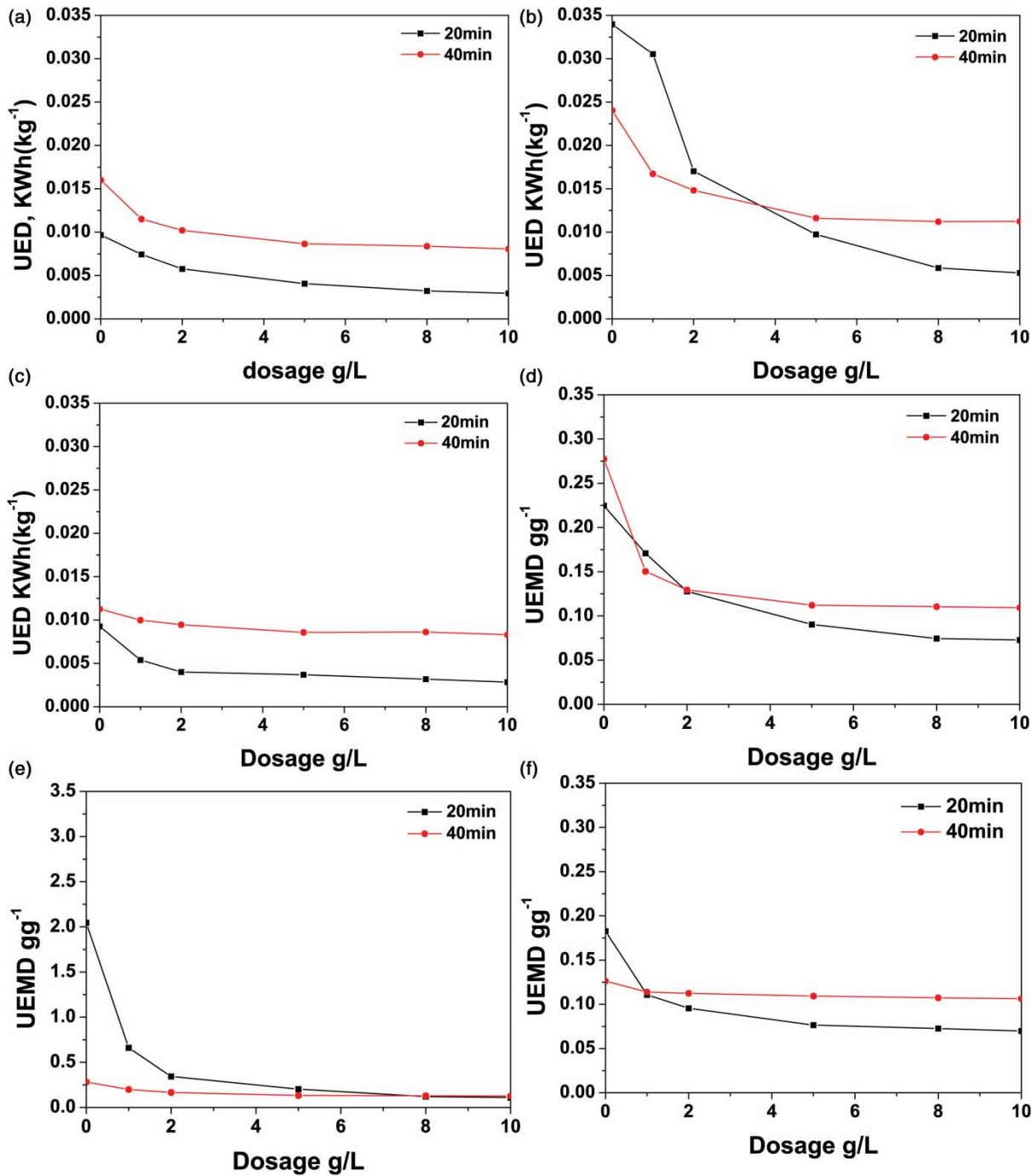


Figure 11 | UED (a) TC, (b) OTC, (c) CTC) and UEMD (d) TC, (e) OTC, (f) CTC with different dosage of PS.

44.37%, respectively. The enhancement of EC + PS system mainly accounts for the synergistic effect of charge neutralization and coordination adsorption. In addition, the sedimentation of flocules produced in EC + PS system

could be promoted by PS, which is conducive to the subsequent solid-liquid separation. This study clearly demonstrated that the EC + PS coupling process is an efficient and cheaper technique for TCs removal.

ACKNOWLEDGEMENTS

We gratefully thank the National Natural Science Foundation of China (No. 41073063).

DATA AVAILABILITY STATEMENT

All relevant data are included in the paper or its Supplementary Information.

REFERENCES

- Antonherrerro, R., Garcíadelgado, C., Alonsoizquierdo, M., Garcíarodríguez, G., Cuevas, J. & Eymar, E. 2017 Comparative adsorption of tetracyclines on biochars and stevensite: looking for the most effective adsorbent. *Applied Clay Science* **298**, 162–172.
- Barhoumi, N., Olvera-Vargas, H., Oturan, N., Huguenot, D., Gadri, A. & Ammar, S. 2017 Kinetics of oxidative degradation/mineralization pathways of the antibiotic tetracycline by the novel heterogeneous electro-Fenton process with solid catalyst chalcocopyrite. *Applied Catalysis B: Environmental* **209**, 637–647.
- Chen, W. & Huang, C. 2010 Adsorption and transformation of tetracycline antibiotics with aluminum oxide. *Chemosphere* **79** (8), 779–785.
- De Carvalho, H. P., Huang, J., Zhao, M., Liu, G., Dong, L. & Liu, X. 2015 Improvement of Methylene Blue removal by electrocoagulation/banana peel adsorption coupling in a batch system. *Alexandria Engineering Journal* **54** (3), 777–786.
- Hernández-Francisco, E., Peral, J. & Blancojerez, L. M. 2017 Removal of phenolic compounds from oil refinery wastewater by electrocoagulation and Fenton/photo-Fenton processes. *Journal of Water Process Engineering* **19**, 96–100.
- Javid, A., Mesdaghinia, A., Nasser, S., Mahvi, A. H., Alimohammadi, M. & Gharibi, H. 2016 Assessment of tetracycline contamination in surface and groundwater resources proximal to animal farming houses in Tehran, Iran. *Journal of Environmental Health Science & Engineering* **14** (1), 4.
- Ji, Y., Shi, Y., Dong, W., Wen, X., Jiang, M. & Lu, J. 2016 Thermo-activated persulfate oxidation system for tetracycline antibiotics degradation in aqueous solution. *Chemical Engineering Journal* **298**, 225–233.
- Jia, S., Yang, Z. & Yang, W. 2016 Removal of Cu(II) and tetracycline using an aromatic rings-functionalized chitosan-based flocculant: enhanced interaction between the flocculant and the antibiotic. *Chemical Engineering Journal* **283**, 495–503.
- Kakavandi, B., Takdastan, A., Jaafarzadeh, N., Azizi, M., Mirzaei, A. & Azari, A. 2016 Application of Fe₃O₄@C catalyzing heterogeneous UV-Fenton system for tetracycline removal with a focus on optimization by a response surface method. *Journal of Photochemistry and Photobiology A-Chemistry* **314**, 178–188.
- Karthikeyan, K. G. & Meyer, M. T. 2006 Occurrence of antibiotics in wastewater treatment facilities in Wisconsin, USA. *The Science of the Total Environment* **361** (1), 196–207.
- Khanday, W. A. & Hameed, B. H. 2018 Zeolite-hydroxyapatite-activated oil palm ash composite for antibiotic tetracycline adsorption. *Fuel* **215**, 499–505.
- Li, Y., Wang, H., Liu, X., Zhao, G. & Sun, Y. 2016 Dissipation kinetics of oxytetracycline, tetracycline, and chlortetracycline residues in soil. *Environmental Science and Pollution Research* **23** (14), 13822–13831.
- Luo, Y., Xu, L., Rysz, M., Wang, Y., Zhang, H. & Alvarez, P. J. 2011 Occurrence and transport of tetracycline, sulfonamide, quinolone, and macrolide antibiotics in the Haihe River Basin, China. *Environmental Science & Technology* **45** (5), 1827–1833.
- Moussa, D. T., Elnaas, M. H., Nasser, M. S. & Almarri, M. J. 2017 A comprehensive review of electrocoagulation for water treatment: potentials and challenges. *Journal of Environmental Management* **186** (1), 24–41.
- Saitoh, T., Shibata, K., Fujimori, K. & Ohtani, Y. 2017 Rapid removal of tetracycline antibiotics from water by coagulation-flocculation of sodium dodecyl sulfate and poly(allylamine hydrochloride) in the presence of Al(III) ions. *Separation and Purification Technology* **187**, 76–83.
- Secula, M. S., Cagnon, B., De Oliveira, T. F., Chedeville, O. & Fauduet, H. 2012 Removal of acid dye from aqueous solutions by electrocoagulation/GAC adsorption coupling: kinetics and electrical operating costs. *Journal of the Taiwan Institute of Chemical Engineers* **43** (5), 767–775.
- Shi, X., Leong, K. Y. & Ng, H. Y. 2017 Anaerobic treatment of pharmaceutical wastewater: a critical review. *Bioresource Technology* **245**, 1238–1244.
- Song, C. 2016 Fate of tetracycline at high concentrations in enriched mixed culture system: biodegradation and behavior. *Journal of Chemical Technology & Biotechnology* **91** (5), 1562–1568.
- Wan, Y., Bao, Y. & Zhou, Q. 2010 Simultaneous adsorption and desorption of cadmium and tetracycline on cinnamon soil. *Chemosphere* **80** (7), 807–812.
- Wang, X., Ni, J., Pang, S. & Li, Y. 2017a Removal of malachite green from aqueous solutions by electrocoagulation/peanut shell adsorption coupling in a batch system. *Water Science and Technology* **75** (8), 1830–1838.
- Wang, Z., Du, Y., Yang, C., Liu, X., Zhang, J., Li, E. & Wang, X. 2017b Occurrence and ecological hazard assessment of selected antibiotics in the surface waters in and around Lake Honghu, China. *Science of the Total Environment* **609**, 1423–1432.
- Wei, M., Gao, L., Li, J., Fang, J., Cai, W., Li, X. & Xu, A. 2016 Activation of peroxymonosulfate by graphitic carbon nitride loaded on activated carbon for organic pollutants degradation. *Journal of Hazardous Materials* **316**, 60–68.
- Xu, Q., Qian, Q., Quek, A., Ai, N., Zeng, G. & Wang, J. 2013 Hydrothermal carbonization of macroalgae and the effects of experimental parameters on the properties of hydrochars.

- ACS Sustainable Chemistry & Engineering* **1** (9), 1092–1101.
- Yan, C., Yang, Y., Zhou, J., Liu, M., Nie, M., Shi, H. & Gu, L. 2013 Antibiotics in the surface water of the Yangtze Estuary: occurrence, distribution and risk assessment. *Environmental Pollution* **175**, 22–29.
- Zhang, F., Yue, Q., Gao, Y., Gao, B., Xu, X., Ren, Z. & Jin, Y. 2017 Application for oxytetracycline wastewater pretreatment by Fenton iron mud based cathodic-anodic-electrolysis ceramic granular fillers. *Chemosphere* **182**, 483–490.
- Zhang, J., Yuan, X., Jiang, L., Wu, Z., Chen, X., Wang, H. & Zeng, G. 2018 Highly efficient photocatalysis toward tetracycline of nitrogen doped carbon quantum dots sensitized bismuth tungstate based on interfacial charge transfer. *Journal of Colloid and Interface Science* **511**, 296–306.

First received 6 May 2020; accepted in revised form 21 July 2020. Available online 5 August 2020